Journal of Pharmacology and Toxicology

ISSN 1816-496X

Academic Journals Inc.

www.academicjournals.com

Journal of Pharmacology and Toxicology 1 (4): 328-336, 2006
ISSN 1816-496X

Molecular Modelling Analysis of the Metabolism of Zaleplon

Fazlul Huq
School of Biomedical Sciences, Faculty of Health Sciences,
The University of Sydney, Australia

Abstract: Zaleplon (ZAL) is a sleep inducing agent with a prompt onset of action. It is rapidly metabolized with 88% of the dose appearing in the urine (71%) and faces (17%) as metabolites. A number of products including M1, M2 and DDZAL are produced from ZAL. M2 is the major metabolite in man whereas DZAL and DDZAL are the major plasma metabolites in rat, mouse and dog. Both M1 and M2 can form glucuronides. Molecular modelling analyses based on molecular mechanics, semi-empirical (PM3) and DFT (at B3LYP/6-31G* level) calculations show that among ZAL and its metabolites, DDZAL has the smallest LUMO-HOMO energy difference so that it would be most kinetically labile. The high kinetic lability and the presence of electron-deficient regions on the molecular surface would make DDZAL the most toxic metabolite as it would react readily with glutathione and nucleobases in DNA. Reaction with glutathione would cause glutathione depletion thus inducing oxidative stress whereas that with nucleobases in DNA would cauase DNA damage.

Key words: Insomnia, zaleplon, sleep-inducing agent, CYP3A, molecular modelling

Introduction

Zaleplon (N-(3-cyanopyrazolo[1,5-a]pyrimidin-7-yl)phenyl]-N-ethylacetamide; CL-288,846; ZAL) is a novel non-benzodiazepine sedative-hypnotic agent used for the treatment of insomnia (Lake *et al*., 2002). It is ultra-short acting sleep inducing agent with a prompt onset of action. Epidemiological studies indicate that approximately one-third of the adult population in the United States suffers from insomnia, ranging from an occasional episode to a chronic condition (Karacan *et al*., 1976; Bixler *et al*., 1979).

After oral administration, ZAL is rapidly absorbed to reach peak plasma concentrations within 1 h. It is a lipophilic compound with a large volume of distribution (1.4 L kg^{-1}) (Beer *et al*., 1994). Although not structurally related to benzodiazepines, ZAL acts through binding to γ-aminobutyric acid ($GABA_A$)-benzodiazepine receptor complex producing sedative and hypnotic effects that are similar to those produced by bezozodiazepines (Mealy and Castaner, 1996).

ZAL is rapidly metabolized (mainly in the liver) with 88% of the dose appearing in the urine (71%) and faces (17%) as metabolites (Wu *et al*., 1996; Rosen *et al*., 1999). A number of products including 5-oxo-ZAL (M2), N-desethyl-ZAL (NDZAL), N-desethyl-5-oxo-ZAL (M1) and 7-(3-aminophenyl)pyrazolo[1,5-a]pyrimidine-3-carbonitrile (DDZAL) (Beer *et al*., 1994; Chaudhary *et al*., 1994; Wu *et al*., 1996; Renwick *et al*., 2002) are produced from ZAL. M2 is the major metabolite in man whereas DZAL and DDZAL are the major plasma metabolites in the rat, mouse and dog (Chaudhary *et al*., 1994). N-deethylation of ZAL to DZAL is NADPH-dependent and catalysed mainly by CYP3A isoforms whereas the metabolism of ZAL to M2 is catalysed by aldehyde oxidase and CYP3A forms in liver cytosol but not in liver microsomes. Both M1 and M2 can form glucuronides. All metabolites of ZAL appear to be pharmacologically inert. M2 and M2-glucuronides account for 57% of the circulating ZAL plasma level (Darwish *et al*., 1999).

In this study molecular modelling analyses have been carried of ZAL and its metabolites in order to obtain a better understanding of toxicity due to ZAL and its metabolites. The study was carried out in the School of Biomedical Sciences, The University of Sydney during February to June 2006.

Computational Methods

The geometries of ZAL and its metabolites have been optimized based on molecular mechanics, semi-empirical and DFT calculations, using the molecular modelling program Spartan '02. Molecular mechanics calculations were carried out using MMFF force field (Fig. 1). Semi-empirical calculations were carried out using the routine PM3. DFT calculations were carried using the program Spartan '02

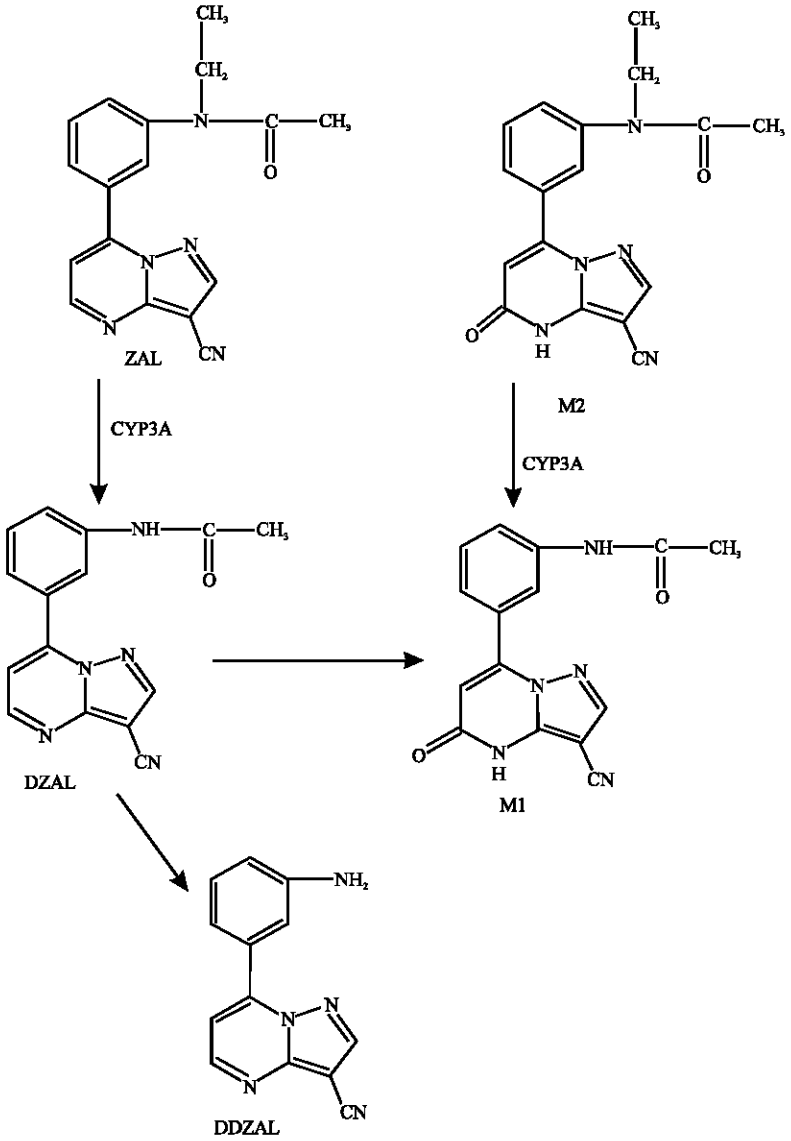

Fig. 1: Metabolic pathways of ZAL (Renwick *et al*., 2002)

at B3LYP/6-31G* level. In optimization calculations, a RMS gradient of 0.001 was set as the terminating condition. For the optimized structures, single point calculations were carried to give heat of formation, enthalpy, entropy, free energy, dipole moment, solvation energy, energies for HOMO and LUMO. The order of calculations: molecular mechanics followed by semi-empirical followed by DFT ensured that the structure was not embedded in a local minimum. To further check whether the global minimum was reached, some calculations were carried out with improvable structures. It was found that when the stated order was followed, structure corresponding to the global minimum or close to that could ultimately be reached in all cases. Although RMS gradient of 0.001 may not be sufficiently low for vibrational analysis, it is believed to be sufficient for calculations associated with electronic energy levels.

Results and Discussion

Table 1 gives the total energy, heat of formation as per PM3 calculation, enthalpy, entropy, free energy, surface area, volume, dipole moment, energies of HOMO and LUMO as per both PM3 and DFT calculations for ZAL and its metabolize M1, M2, DZAL and DDZAL. Figure 2-6 give the regions of negative electrostatic potential (greyish-white envelopes) in (a), HOMOs (where red indicates HOMOs with high electron density) in (b), LUMOs in (c) and density of electrostatic potential on the molecular surfaces (where red indicates negative, blue indicates positive and green indicates neutral) in (d) as applied to the optimized structures of ZAL and its metabolites M1, M2, DZAL and DDZAL.

The calculated solvation energies of ZAL and its metabolites M1, M2, DZAL and DDZAL from PM3 calculations in kcal mol^{-1} are respectively -11.89, -14.93, -11.69, -14.22 and -11.83 and their dipole moments from DFT calculations are 7.9, 4.2, 5.7, 5.3 and 8.3, respectively. The values suggest that ZAL and its metabolites would have low solubility in water.

Table 1: Calculated thermodynamic and other parameters of ZAL and its metabolites

Molecule	Calculation type	Total energy (kcal mol^{-1}/ atomic unit*)	Heat of formation (kcal mol^{-1})	Enthalpy (kcal mol^{-1} K^{-1})	Entropy (cal mol^{-1} K^{-1})	Solvation energy (kcal mol^{-1} K^{-1})	Free energy (kcalmol^{-1})
ZAL	PM3	83.930	95.81	197.36	149.27	-11.89	152.86
	DFT	-1005.800		198.12	148.74	-13.15	153.80
M1	PM3	86.530	101.46	160.54	136.68	-14.93	119.79
	DFT	-1002.430		161.13	136.03	-16.67	120.59
M2	PM3	31.720	43.41	201.04	155.97	-11.69	154.54
	DFT	-1081.040		201.93	155.15	-12.95	155.70
DZAL	PM3	101.280	87.06	160.33	136.28	-14.22	119.69
	DFT	-927.190		161.14	135.67	-16.23	120.71
DDZAL	PM3	129.333	141.16	135.41	118.76	-11.83	100.00
	DFT	-774.530		136.08	118.00	-13.10	100.92

Molecule	Calculation type	Area ($Å^2$)	Volume ($Å^3$)	Dipole moment (debye)	HOMO (eV)	LUMO (eV)	LUMO-HOMO (eV)
ZAL	PM3	334.23	314.28	6.8	-9.25	-1.39	7.86
	DFT	330.64	312.38	7.9	-6.33	-2.29	4.04
M1	PM3	298.88	277.21	5.5	-9.30	-1.43	7.87
	DFT	303.05	282.49	4.2	-6.48	-2.13	4.35
M2	PM3	339.46	320.51	4.4	-9.14	-1.29	7.85
	DFT	340.39	320.06	5.7	-6.45	-2.10	4.35
DZAL	PM3	296.60	276.37	4.8	-9.21	-1.38	7.83
	DFT	293.27	274.92	5.3	-6.39	-2.32	4.07
DDZAL	PM3	254.93	235.59	6.3	-9.02	-1.32	7.70
	DFT	250.66	233.91	8.3	-6.00	-2.16	3.84

* in atomic units from DFT calculations

The LUMO-HOMO energy differences for ZAL and its metabolites are found to range from 3.84 to 4.35 indicating that the compounds would differ in their kinetic lability. DDZAL is found to be most labile followed by ZAL. The molecular surfaces of ZAL and its metabolites (Fig. 2d-6d) are found to have electron-rich (red), electron-deficient (blue) and neutral (green) regions so that they may be subject to electrophilic, nucleophilic and hydrophobic interactions. The surface of ZAL is found to abound most in electron-deficient regions followed by that of DDZAL. This means that ZAL and DDZAL may react readily with cellular glutathione and nucleobases in DNA, thus causing

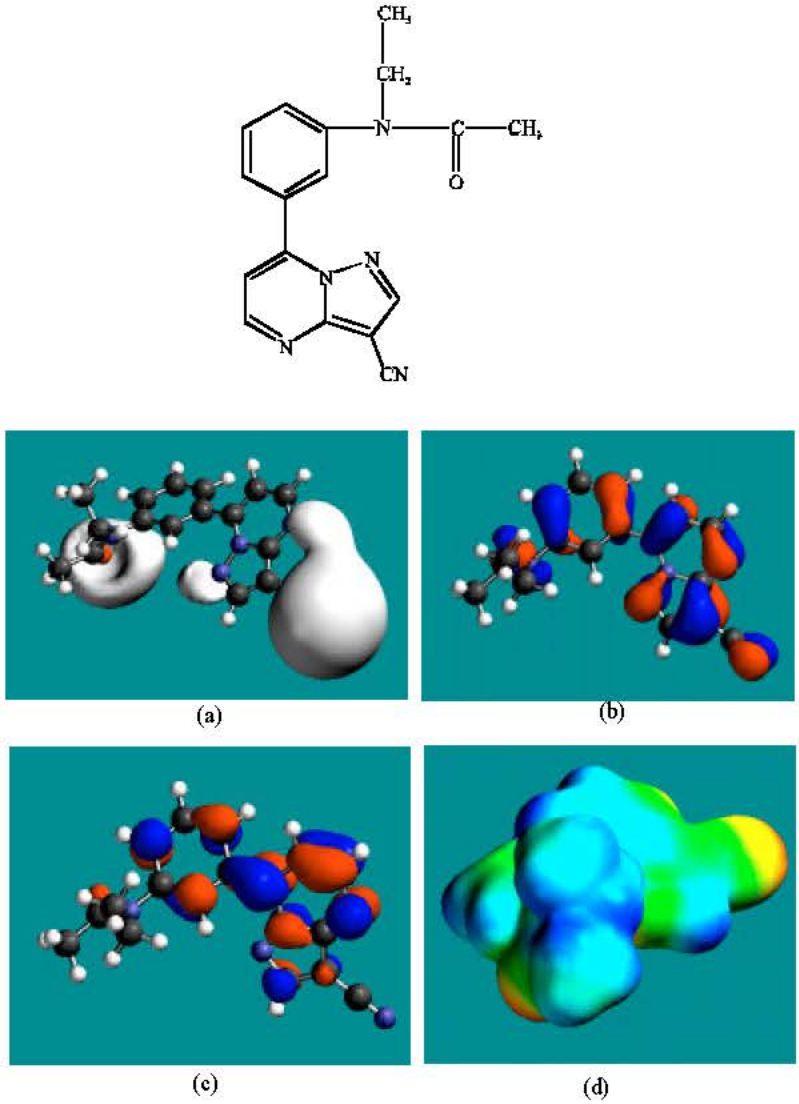

Fig. 2: Structure of ZAL giving in: (a) the electrostatic potential (greyish envelope denotes negative electrostatic potential), (b) the HOMOs, (where red indicates HOMOs with high electron density) (c) the LUMOs (where blue indicates LUMOs) and in (d) density of electrostatic potential on the molecular surface (where red indicates negative, blue indicates positive and green indicates neutral)

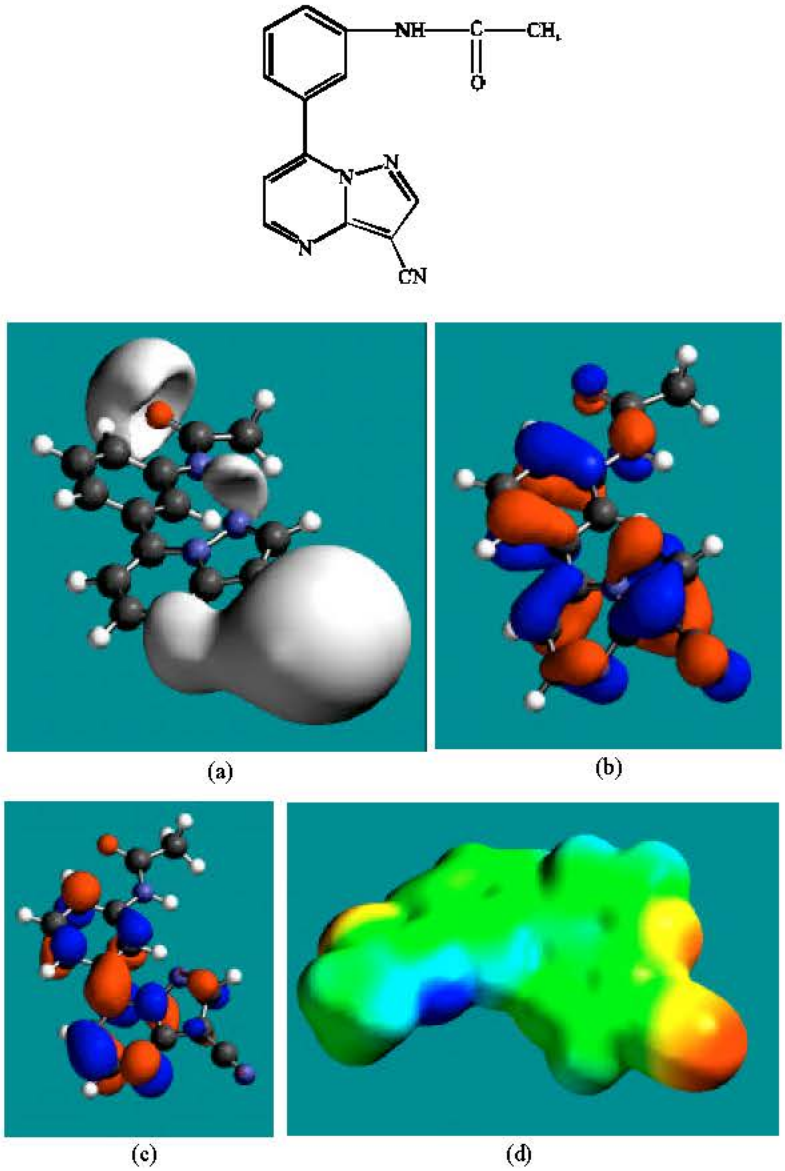

Fig. 3: Structure of DZAL giving in: (a) the electrostatic potential (greyish envelope denotes negative electrostatic potential), (b) the HOMOs, (where red indicates HOMOs with high electron density) (c) the LUMOs (where blue indicates LUMOs) and in (d) density of electrostatic potential on the molecular surface (where red indicates negative, blue indicates positive and green indicates neutral)

glutathione depletion and oxidation of nucleobases in DNA. Depletion of glutathione introduces oxidative stress by compromising the antioxidant status of the cell whereas the oxidation of nucleobases in DNA causes DNA damage.

In the case of ZAL, DZAL, M1 and M2, the electrostatic potential is found to be more negative around the carbonyl oxygen and various nitrogen centres indicating that the positions may be subject

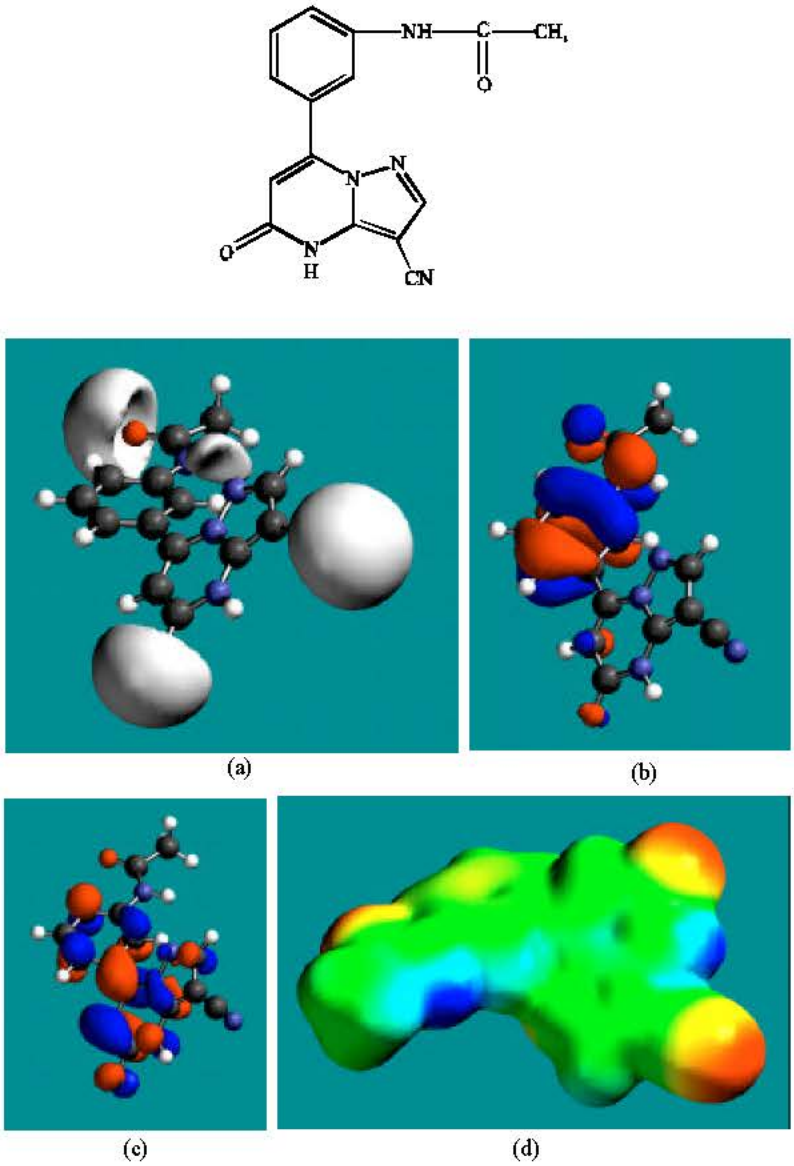

Fig. 4: Structure of M1 giving in: (a) the electrostatic potential (greyish envelope denotes negative electrostatic potential), (b) the HOMOs, (where red indicates HOMOs with high electron density) (c) the LUMOs (where blue indicates LUMOs) and in (d) density of electrostatic potential on the molecular surface (where red indicates negative, blue indicates positive and green indicates neutral)

to electrophilic attack. In the case of DDZAL, the electrostatic potential is found to be more negative around the various nitrogen centres indicating that the positions may be subject to electrophilic attack.

In the case of ZAL, the HOMOs with high electron density are found close to the non-hydrogen atoms of the two phenyl rings whereas the LUMOs are found close to the atoms of the amino side chain. In the case of AcMAP, HOMOs with high electron density and LUMOs are found close to the

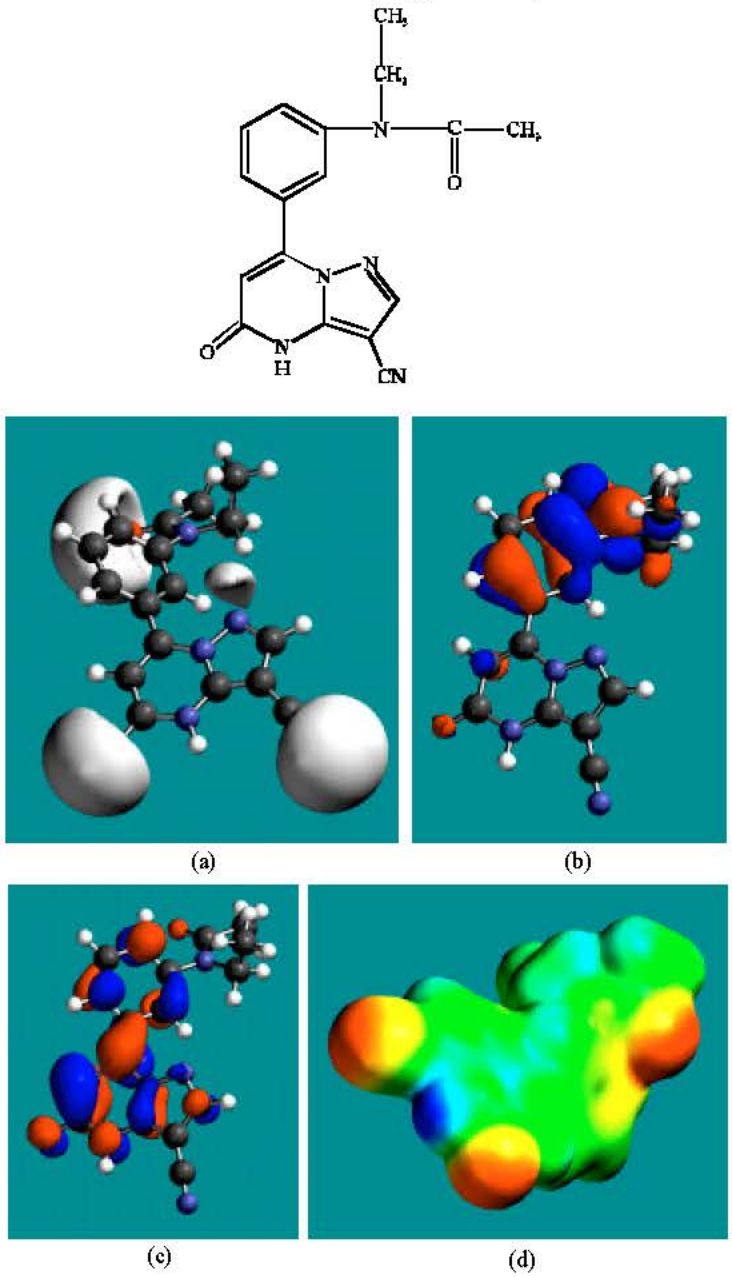

Fig. 5: Structure of M2 giving in: (a) the electrostatic potential (greyish envelope denotes negative electrostatic potential), (b) the HOMOs, (where red indicates HOMOs with high electron density) (c) the LUMOs (where blue indicates LUMOs) and in (d) density of electrostatic potential on the molecular surface (where red indicates negative, blue indicates positive and green indicates neutral)

non-hydrogen atoms of the two phenyl rings. The overlap of HOMO with high electron density and region of negative electrostatic potential close to sulfur, gives further support to the idea that the position may be subject to electrophilic attack.

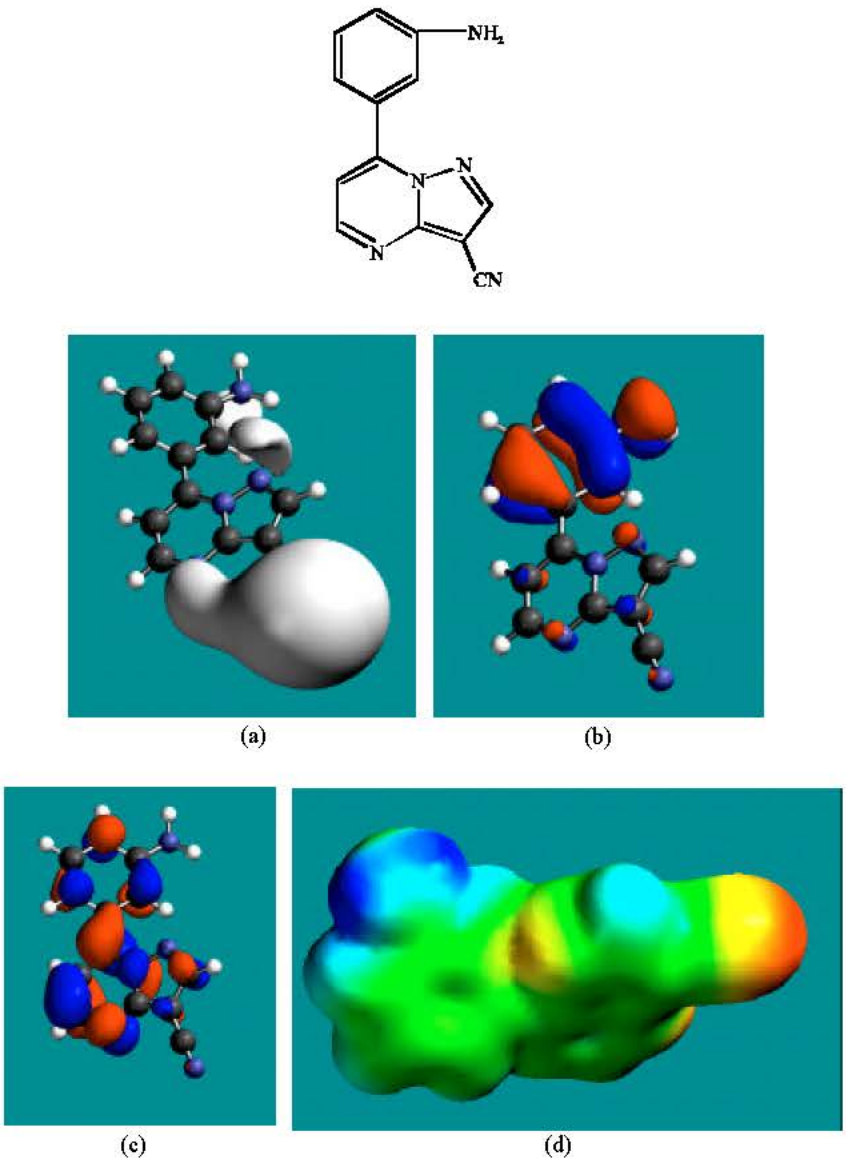

Fig. 6: Structure of DDZAL giving in: (a) the electrostatic potential (greyish envelope denotes negative electrostatic potential), (b) the HOMOs, (where red indicates HOMOs with high electron density) (c) the LUMOs (where blue indicates LUMOs) and in (d) density of electrostatic potential on the molecular surface (where red indicates negative, blue indicates positive and green indicates neutral)

When surface area and volume of ZAL are compared with those of its metabolites DZAL, M1, M2 and DDZAL, it is found to that the values of M2 are comparable to those of ZAL (Table 1). Since none of the metabolites of ZAL is found to be pharmacologically active, it is suggested that M2, in spite of having similar surface area and volume as those of ZAL, cannot be substrate for the binding site in the $GABA_A$ receptor suggesting that the carbonyl group in M2 must be a deterrent to binding.

Conclusion

Molecular modelling analyses based on semi-empirical and DFT calculations show that among ZAL and its metabolites, DDZAL has the smallest LUMO-HOMO energy difference so that it would be most labile. The high lability and the presence of electron-deficient regions on the molecular surface means that DDZAL would react most readily with glutathione and nucleobases in DNA, thus inducing cellular toxicity and DNA damage.

Acknowledgment

Fazlul Huq is grateful to the School of Biomedical Sciences, The University of Sydney for the time release from teaching.

References

Beer, B., J.R. Jeni, W.H. Wu, D. Clody, P. Amorusi and J. Rose *et al*., 994. A placebo-controlled evaluation of single, escalating doses of CL 284,846 (zaleplon), a non-benzodiazepine hypnotic. J. Clin. Pharmacol., 34: 335-344.

Bixler, E.O., A. Kales, C.R. Soldatos, J.D. Kales and S. Healey, 1979. Prevalence of sleep disorders in the Los Angeles metropolitan area. Am. J. Psychiatr., 136: 1257-1262.

Chaudhary, I., W. Demalo and J. Kantrowitz, 1994. Species comparison of *in vitro* and *in vivo* metabolism of CL-284,846, a non-benzodiazepine sedative/hypnotic agent. Pharmaceut. Res., 11: S391.

Darwish, M., P.T. Martin, W.H. Cevallos, S. Tse, S. Wheeler and S.M. Troy, 1999. Rapid disappearance of zaleplon from breast milk after oral administration to lactating women. J. Clin. Pharmacol., 39: 670-674.

Karacan, I., J.I. Thornby, M. Anch, C.E. Holzer, G.J. Warheit, J.J. Schwab and R.L. Williams, 1976. Prevalence of sleep disturbance in a primary urban Florida county. Soc. Sci. Med., 10: 239-244.

Lake, B.G., S.E. Ball, J. Kao, A.B. Renwick, R.J. Price and J.A. Scatina, 2002. Metabolism of zaleplon by human liver: Evidence for involvement of aldehyde oxidase. Xenobiotica, 32: 835-847.

Mealy, N and J. Castaner, 1996. Zaleplon, a new sedative/hypnotic. Drugs of the Future, 21: 37-39.

Renwick, A.B., S.E. Ball, J.M. Tredgers, R.J. Price, D.G. Walters, J. Kao, J.A. Scatina and B.G. Lake, 2002. Inhibition of zaleplon metabolism by cimetodine in the human liver: *In vitro* studies with subcellular fractions and precision-cut liver slices. Xenobiotica, 32: 849-862.

Rosen, A.S., P. Fournie, M. Darwish, P. Danjou and S.M. Trov, 1999. Zaleplon pharmacokinetics and absolute bioavailability. Biopharmaceutics and Drug Dispos., 20: 171-175.

Spartan '02, 2002. Wavefunction, Inc. Irvine, CA, USA.

Wu, W.H., A.T. Dicioccio, W. Demaio, P. Amorusi, A.P. Tonelli and P.R. Mayer, 1996. Mass balance and pharmacokinetics of zaleplon, a non-benzodiazepine sedative/hypnotic, in man. Pharmaceut. Res., 13: S487.